
Identifiable Latent Bandits: Leveraging observational data for personalized decision-making

Ahmet Zahid Balcioglu
 Chalmers University of Technology
 University of Gothenburg
 ahmet.balcioglu@chalmers.se

Newton Mwai
 Chalmers University of Technology
 University of Gothenburg

Emil Carlsson
 Sleep Cycle

Fredrik D. Johansson
 Chalmers University of Technology
 University of Gothenburg

Abstract

For many decision-making tasks, such as precision medicine, historical data alone are insufficient to determine the right choice for a new problem instance or patient. Online algorithms like multi-armed bandits can find optimal personalized decisions but are notoriously sample-hungry. In practice, training a bandit for a new individual from scratch is often infeasible, as the number of trials required is larger than the practical number of decision points. Latent bandits offer rapid exploration and personalization beyond what context variables can reveal, provided that a latent variable model can be learned consistently. In this work, we propose an identifiable latent bandit framework that leads to optimal decision-making with a shorter exploration time than classical bandits by learning from historical records of decisions and outcomes. Our method is based on nonlinear independent component analysis that provably identifies representations from observational data sufficient to infer the optimal action in new bandit instances. We verify this strategy in simulated and semi-synthetic environments, showing substantial improvement over online and offline learning baselines when identifying conditions are satisfied.

1 Introduction

The goal of personalized decision-making is to find the actions best suited for specific individuals. For example, chronic diseases such as rheumatoid arthritis have dozens of therapy options after diagnosis [48, 32] whose efficacy for a new patient are unknown, and would need to be tried out sequentially, until an optimal match is found. Online sequential decision-making of this form has been extensively studied in the multi-armed bandit (MAB) literature [50, 39, 8], but bandit algorithms often require orders of magnitude more trials to converge than a patient could practically go through, precluding the use of bandit algorithms in personalized medicine [20].

A pragmatic solution to minimize the sample complexity in personalized decision-making is to leverage (offline) observational data of previous decisions and outcomes [40]. For example, estimating conditional causal effects [41, 47, 23, 10] from cross-sectional or longitudinal observational data allows decision-makers to tailor choices to a set of context variables. However, a single set of context variables observed passively before making decisions is usually insufficient to identify an optimal *personalized* action.

Paradigms blending online and offline learning have been proposed to shorten exploration. For instance some bandit algorithms exploit the structure between a *context variable*, actions, and rewards

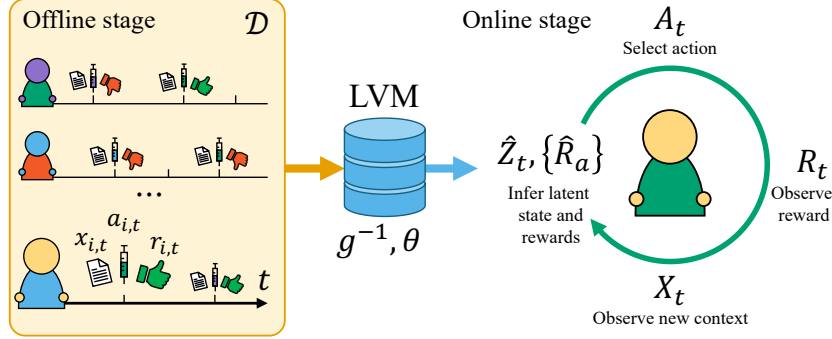


Figure 1: Identifying the best treatment for a new patient using ILB. In the offline stage, we use the results from Theorem 3.3 to learn an LVM that identifies the latent state and show in Theorem 3.4 how such a model enables learning the reward model. For decision-making algorithms see Algorithm 1.

to personalize decisions [6, 1, 56, 25]. They can be further improved in the offline stage by either warm-starting model parameters for online learning by learning from historical data in an offline phase [54, 33, 34], or leveraging historical data to reveal structure about the data through observable or latent clustering [5, 4, 30, 15, 20, 16], matrix decomposition [46], or spectral methods [22, 42].

When the latent structure is known prior to the online phase, *latent bandits* [15, 20] have proved theoretically and empirically more sample efficient than unstructured bandits, but leave a question open: How can we learn such latent structure from data and when will it lead to optimal decision making? Provable recovery of such latent structure is the goal of identifiable representation learning. Common approaches make structural assumptions about the data such as independent latent components [17] or causal structure of the data generation process [44], and make use of methods like normalizing flows [38], or contrastive learning [9]. In this work, we build on these developments to learn identifiable representations to improve personalized decision-making.

Contributions. (1) We introduce *identifiable latent bandits*, the first family of latent bandit algorithms that recover a continuous vector-valued latent state without requiring the latent variable model (LVM) to be known a priori. (2) We build on nonlinear independent component analysis (ICA) [7] for identifiable representations and introduce mean-contrastive learning and use it to provably learn the LVM. (3) We prove that this framework is partially identifiable to a degree sufficient for optimal decision-making and propose three algorithms that exploit the latent variable model for personalized sequential decision-making in the regret minimization setting. (4) We show in experiments that, when the conditions of our theory hold, our algorithms are more sample-efficient than online bandits, less biased than offline (regression) baselines, and preferable to hybrid alternatives, both when a perfect (oracle) model is used and when the LVM has been learned from observational data. We test the sensitivity of our algorithm to various violated assumptions and demonstrate its efficacy in a semi-synthetic environment for choosing a therapy for patients with Alzheimer’s disease [21].

2 Problem setup

Treatment of chronic diseases like rheumatoid arthritis and Alzheimer’s disease is differential and symptomatic. Most patients go through a long, sequential decision-making process before finding the best therapy option for them [48, 32, 49]. Minimizing suffering throughout this process is crucial.

We use the choice of medical treatment as a running, motivating example and model the decision-making process for a patient (problem instance) $i \in \mathbb{N}$ who is given treatments (actions) $A_{i,t} \in \mathcal{A} = \{1, \dots, K\}$ over rounds $t = 1, \dots, T$, resulting in observed stochastic rewards $R_{i,t} \in \mathbb{R}$ with means μ_{i,a_t} . At each round, a decision-maker observes a set of context variables $X_{i,t} \in \mathbb{R}^d$ and aims to select an action $A_{i,t}$ based on the history $H_{i,t} = (X_{i,s}, A_{i,s}, R_{i,s})_{s=1}^{t-1}$ and the current context $X_{i,t}$, to minimize the cumulative regret (Reg_T) [25],

$$\text{Reg}_T = \mathbb{E} \left[\mu_i^* - \sum_{t=1}^T R_{i,t} \right] \quad \text{where} \quad \mu_i^* = \mu_{i,a^*}, \quad (1)$$

with $a_i^* = \arg \max_{a \in [K]} \mu_{i,a}$ the optimal action for the current problem instance. Without further assumptions, achieving small regret typically requires prohibitively many trials to learn the reward distributions for a new instance [11]. To mitigate this, we exploit *shared structure* between the rewards of different instances so that previous instances can inform the solutions of future ones.

We assume the rewards are structured according to a *latent variable* $Z_i \in \mathbb{R}^n$, constant in time for each instance i , which fully determines the reward distribution of each action. Consequently, any two instances i, j with the same latent state $z_i = z_j = z$ share expected rewards of actions $\mu_{i,a} = \mu_{j,a} = \mu_a(z)$, and optimal arms. The same assumption is central to *latent bandits* [31, 46, 20, 15]. The key components of latent bandit algorithms are a latent variable model (LVM) approximating $p(Z_i | H_{i,t}, X_{i,t})$ and a reward model $\mu_a(z)$ for each value of z , used to select the next action using a *selection criterion* based on an inferred value of Z . For example, the mTS algorithm [15] samples $\hat{z}_t \sim p(Z_i | H_{i,t}, X_{i,t})$ and selects the action $a_t = \arg \max_a \mu_a(\hat{z}_t)$. However, this and related works assume that both models are known a priori but give little guidance for how to learn or acquire them. To make real-world application plausible, we posit that algorithms must learn the LVM from *observational historical data* $\mathcal{D} = \{(x_{1,t}, a_{1,t}, r_{1,t})_{t=1}^{T_1}, \dots, (x_{I,t}, a_{I,t}, r_{I,t})_{t=1}^{T_I}\}$ of I previous problem instances, each with a sequence length $T_i, i \in [I]$. This presents a first new problem: not all LVMs are *identifiable*—they may fail to recover the true underlying process that generated \mathcal{D} [17].

We view the reward of an action a as the causal effect of an intervention $\mathbf{do}(A_t = a)$ [35] on the instance (patient), and define $\mu_a(z) := \mathbb{E}[R | \mathbf{do}(A_t = a), Z = z]$, where the \mathbf{do} -notation of Pearl [35] distinguishes intervening from conditioning on the action A_t . This distinction is critical when learning $\mu_a(z)$ from observational data as this faces threats of confounding and other biases [35]. For example, if different patients represented in \mathcal{D} were given systematically different treatments depending on an unobserved variable, $\mathbb{E}[R_t | \mathbf{do}(A_t = a), Z = z] \neq \mathbb{E}[R_t | A_t = a, Z = z]$ in general. Thus, to apply a latent bandit algorithm in online decision-making, we must first show that

$$\text{i) } p(Z | H_t, X_t) \quad \text{and} \quad \text{ii) } \mu_a(z) = \mathbb{E}[R_t | \mathbf{do}(A_t = a), Z = z] . \quad (2)$$

can be identified and estimated from \mathcal{D} :

The central goal of this work is to (i) design an algorithm that learns an *identifiable* model of the latent variable Z and the rewards of actions $\mu_a(z)$ from observational data \mathcal{D} during an *offline* phase, and (ii) prove that it leads to personalized, *online* sequential decision-making algorithms with lower sample complexity than algorithms that ignore \mathcal{D} .

2.1 Additional related work

Contextual bandits [6, 1, 56, 25] exploit structure in the rewards of actions by parameterizing their distribution as a function $\mu_a(x)$ of an observed context, x and apply these parameters in new contexts. The problem is distinct from ours and has a different goal. In contextual bandits, each context x is associated with a potentially different optimal action and reward distribution. In our setting, the optimal action is the same in each round $t = 1, \dots, T$, and a single context X_t at any one round t is insufficient to fully determine the optimal action. Thus, *contextual bandits do not solve our problem*. We give a closer comparison of latent and contextual bandits in the Appendix F.

A large branch of causal inference research aims to estimate conditional causal effects of actions (CATE) from observational (offline) data to support future decision-making [36, 2, 53]. Representation learning can be used to predict causal effects more accurately by embedding high-dimensional covariates and actions in a space that reveals causal relations [47, 45, 52] and latent variable models [28, 37, 29, 55] can be used to recover from confounding due to unobserved variables by exploiting assumptions on the data generating process. Previous work viewing bandits as online causal effect estimators [24, 26, 3, 28] have also mostly focused on remedying the effects of unobserved confounders. However, unobserved confounding is not a focus here, and these works are not concerned with sample-efficient online decision-making.

3 Identifiable latent bandits

In this section, we give a two-stage latent bandit algorithm that combines offline and online learning to perform optimal personalized decision-making in the online stage. We prove that, under the right

conditions (3.1), both a latent variable model (3.2) and decision-making criteria (3.2.1), can be learned from observational data in the offline stage. We use these results to give provably efficient sequential decision-making algorithms (3.3) for new problem instances in the online stage. We illustrate this approach, dubbed *identifiable latent bandits* (ILB), in Figure 1.

3.1 Identifying assumptions on the data-generating process

Our assumptions are motivated by the problem of finding the right symptomatic treatment for patients with a chronic diseases, such as rheumatoid arthritis. For such conditions, drugs only affect symptoms and can't cure the disease (Z is constant in time), and both symptoms and responses vary with time in unpredictable ways (X_t, R_t are noisy). This means that a single trial of each treatment candidate is not sufficient to identify the optimal personalized treatment for a given patient [12]. Finally, we assume the response to treatment for a subject is stationary and determined up to exogenous noise by their subtype Z , $p(R_t | Z, \text{do}(A_t = a)) = p(R'_t | Z, \text{do}(A'_t = a))$. This is plausible for conditions that don't progress more rapidly than treatment exploration can be performed. We give a formalization of our identifying assumptions below.

Assumption 3.1 (Identifying assumptions). As illustrated in Figure 2, we assume that

- (a) Each instance i is generated by the following structural equations, for all $t \in [T_i]$,

$$\begin{aligned} Z_i &= U & Z_{i,t} &= Z_i + \eta_{i,t} \\ X_{i,t} &= g(Z_{i,t}) & R_{i,t} &= \theta_A(Z_i) + \epsilon_{A_{i,t}} \end{aligned} \quad (3)$$

where $\eta_{i,t} \sim \mathcal{N}(\mathbf{0}, \sigma^2 \mathbb{I})$ and thus, each source variable $Z_{i,t} \in \mathbb{R}^n$ is stationary in time with respect to the instance $i \in [I]$.

- (b) U follows a non-parametric product distribution p_u
(c) The nonlinear transform g , referred to as the *emission function*, is smooth and invertible.
(d) Rewards are generated according to a function θ_A with $\epsilon_{A_{i,t}}$ sub-Gaussian noise with mean zero and parameter σ_i .

We make no assumptions on the distribution of actions $A_{i,t}$ other than the causal (and probabilistic) independencies indicated in Figure 2. We assume that θ is a linear transformation for most of the discussion and simply denote it as a matrix. We investigate the nonlinear case empirically (see Appendix E.4). We assume Gaussianity of $\eta_{i,t}$ for the convenience of further arguments; in fact, $\eta_{i,t}$ can be any mean-zero exponential family noise (see Appendix B).

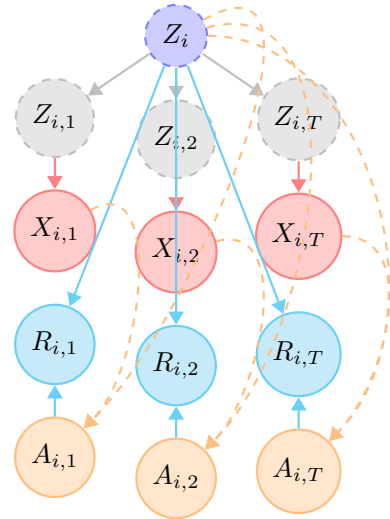


Figure 2: The structural causal model of Assumption 3.1 for an example patient instance i . Dashed arrows indicate potential sources of confounding bias that our model can handle.

Assumptions in related work. Our assumptions on g are relaxed compared to some previous work on latent bandits [46, 22], to allow for nonlinear functions and continuous latent states. Assumption 3.1 c) is more typical of the literature on nonlinear ICA [17] and is a necessary but not sufficient condition for the recovery of Z . However, by Assumption (3.1) a), each instance differs in mean, as opposed to in noise, which is the standard assumption in ICA literature [18]. To emphasize this, we call the resulting contrastive learning algorithm *mean-contrastive*. In [15] the authors assume implicitly that the context variable is marginally independent of the latent state, but that rewards depend directly on the context. Thus, the context alone is not useful for inferring the latent state. This is distinct from our setting where context and rewards are determined by Z_i and are conditionally independent given Z_i .

Under Assumption 3.1, the set of expected rewards is determined by the latent state through $\theta_A(z_i)$ per equation (3). Consequently, if θ_A is known, it is sufficient to infer z_i to make an optimal decision for patient i . As we will see next, the assumption that context variables $X_1 \dots, X_t$ are generated from a noisy Z through an *invertible* transform supports precisely this strategy.

3.2 Offline stage: Identifying and estimating the latent variable model

In the *offline stage* of the ILB algorithm (Algorithm 1), we learn the inverse emission function g^{-1} and reward model θ from the observational data \mathcal{D} to support inferring the latent state Z_i and the best possible action for a new instance i . To fit g^{-1} , we use contrastive learning with multinomial logistic regression [17] where we learn from observed contexts $x_t \in \mathcal{D}$, stripped of instance identifiers, to predict to which instance $c \in [I]$ an observation belongs. We fit a deep feature extractor $f \in \mathbb{R}^n$, with parameters, and a multinomial logistic regression model with softmax activation logits over classes c given by $q_c(f(x)) = W_c^\top f(x) + b_c$, yielding the classifier

$$p(C = c \mid X = x; W, b) = \frac{e^{q_c(f(x))}}{1 + \sum_{j=2}^I e^{q_j(f(x))}}, \quad (4)$$

where C is the instance indicator and $W_c \in \mathbb{R}^d$ and $b_c \in \mathbb{R}^d$ are instance-specific weights and biases respectively. We say that a feature extractor f^* is optimal if there is a classifier based on f^* that maximizes the expected log-likelihood,

$$f^*, q^* = \arg \max_{f, q} \sum_{i=1}^I \sum_{t=1}^{T_i} \log \left[\frac{e^{q_i(f(x_{i,t}))}}{1 + \sum_{j=2}^I e^{q_j(f(x_{i,t}))}} \right] \quad (5)$$

As the number of observations per instance approaches infinity ($\lim T_i \rightarrow \infty, \forall i \in [I]$), a universal function approximator on the form of (4) with feature extractor f^* that maximizes the empirical log-likelihood in (5) will converge to the true posterior $p(C \mid X)$, see Lemma B.1 in Appendix B.

For the learning of such a feature extractor and classifier to be viable, we make the following assumptions:

Assumption 3.2 (Viable learning task). We assume the following of the learning problem in (5).

- (a) The dimension of the latent state is known and equal to the feature extractor f i.e. $n = d$.
- (b) The matrix of patient latent states in for instances in \mathcal{D} , $M = [z_1, \dots, z_I]^\top \in \mathbb{R}^{n \times I}$ has rank n ; that is, patients are sufficiently distinct.

Assumption 3.2 (a) is a simpler statement of our earlier assumption Assumption 3.1 (c) of invertibility of the data generating process. The second assumption relates to the variation of instances in the dataset, as we can not expect to fully recover the latents if the variation is not reflected in the dataset. We can now state our identifiability result.

Theorem 3.3 (Identifiability of inverse emission function). *Under Assumptions 3.1–3.2, in the limit of infinite per-instance data, the optimal feature extractor f^* , according to (5), is equal to the inverse emission function g^{-1} up to an invertible affine transformation. In other words,*

$$Bf^*(x) + b = g^{-1}(x) \quad (6)$$

for constant invertible matrix $B \in \mathbb{R}^{d \times d}$, and vector $b \in \mathbb{R}^d$.

We give the proof of Theorem 3.3 in Appendix B.1. The result partially identifies $p(Z \mid H_t, X_t)$, (i) in (2), as the distribution of the true latent state $Z = z$ is Gaussian around the inverse emission function g^{-1} by Assumption 3.1, i.e. $z = \mathbb{E}[g^{-1}(X_t) \mid Z = z]$. Such affine identifiability results are common in the non-linear ICA literature and make extensive use of the parametric form of the latent distribution [17, 19]. Fitting f by solving (5) forms the first step of Algorithm 1.

3.2.1 Identifiability of reward model and decision-making criteria

Once the feature extractor f has been learned, we can estimate the reward model θ_a for each action a using regression fit to input-output pairs $(f(x_t), r_t)$ for observations $(x_t, a_t, r_t) \in \mathcal{D}$ where $a_t = a$. This forms step 2 of Algorithm 1. Theorem 3.3 only guarantees that f is an accurate model of g^{-1} up to an affine transform. However, as we prove below, when reward means are linear, up-to-affine identifiability of $g^{-1}(x_t)$ is sufficient for this procedure to identify $\mathbb{E}[R_{i,t} \mid Z_i = z, \text{do}(A_{i,t} = a)]$.

Theorem 3.4. *Assume that reward means are linear, $\mu_a(z) = \theta_a^\top z$, and fix a problem instance i . Then, under the conditions of Assumption 3.1, the state-conditional expected reward $\mathbb{E}[R_{i,t} \mid Z_i = z, \text{do}(A_{i,t} = a)]$ of an intervention a is identifiable from the observational distribution of problem instances $p(H_T)$ by the OLS regression estimand applied to observed rewards and latent states inferred by an optimal feature extractor f in the sense of Theorem 3.3.*

Algorithm 1 Identifiable latent bandits (ILB) with CPG and FPG decision-making criteria

Observational data: Learn LVM

- 1: Use observational data $\{(x_{i,t}, c_{i,t})\}_{i \in [I], t \in [T_i]}$ with $c_{i,t} := i$ the instance index to train the contrastive learning model f .
- 2: Fit $\hat{\theta}$ to inferred latent states $\bar{z}_{i,t}$ and rewards in \mathcal{D} using OLS.

Decision-making time: Infer Z , act greedily

- 1: **for** $t = 1, \dots, T$ **do**
 - 2: Observe $x_{i,t}$
 - 3: Use LVM estimate latent variable $\hat{z}_{i,t} = f(x_{i,t})$,
 - 4: **if** CPG: Update belief about latent state
 $\hat{z}_i = \hat{\mathbb{E}}[\hat{z}_{i,t}] := \frac{1}{t} \sum_{t'=1}^t f(x_{t'})$
 - 5: **if** FPG: Update belief about latent state
 $\hat{z}_i = \arg \min_z \left[\sum_{t'=1}^t (r_{i,t'} - \hat{\theta}_{a_{i,t'}}^\top z)^2 + \|z - \hat{\mathbb{E}}[\hat{z}_{i,t}]\|^2 \right] \quad (7)$
 - 6: **if Greedy:**
 - 7: Estimate reward means, $\hat{\mu}_a = \hat{\theta}_a^\top \hat{z}_i$.
 - 8: **if Exploration:** (for FPG only)
 - 9: Sample reward means, $\hat{\mu}_a \sim \mathcal{N}(\theta_a^\top \hat{z}_i, \hat{\theta}_a^\top V^{-1} \theta_a)$, for $V = \sum_{t'=1}^t \hat{\theta}_{a_{t'}} \hat{\theta}_{a_{t'}}^\top$.
 - 10: Choose next action as $a_{i,t} = \arg \max_{a \in \mathcal{A}} \hat{\mu}_a$ and observe reward $r_{i,t}$
 - 11: **end for**
-

The proof of Theorem 3.4 is given Appendix C. It follows three steps where we first show the causal identifiability of the reward model, and generalize it to the cases when Z is estimated via the oracle inverse emission function g^{-1} , and the feature extractor f optimizing (5). We use the result to derive the action selection criteria on lines 7 and 9 in Algorithm 1.

3.3 Online stage: Estimation of the latent state & decision making

The results in Theorems 3.3–3.4 allow for an unbiased estimation of the rewards for each arm through a estimation of the latent state $\hat{\mu}_{i,a} = \hat{\theta}_a^\top \hat{z}_i$. In Algorithm 1, we present two different approaches for exploiting the learned LVM to *estimate* the (posterior distribution of the) latent state and show how our method allows for *exploration* in the decision-making.

A single context $x_{i,t}$ is noisy and does not carry enough information to accurately infer the instance-specific latent state z_i . However, under the conditions of Theorem 3.3, with an inference function f that is optimal w.r.t. (5), $\bar{z}_{i,t} = \sum_{t'=1}^t f(x_{i,t'})/t$ is an unbiased estimate of the latent variable z_i , up to a constant affine transform. Moreover, Theorem 3.4, justifies estimating $\theta^\top z$ by a linear model fit to \bar{z} . Thus, for a well-specified and well-estimated LVM, an intuitive approach is to play the best arm given the current estimate \bar{z}_i and previously estimated reward parameters $\hat{\theta}$ at each time-step, $a_t = \arg \max_{a \in \mathcal{A}} \theta_a^\top \bar{z}_{i,t}$. We call this model *context posterior greedy* (CPG), as it uses only the context variables for posterior inference.

Notably the CPG does not exploit the dependence of rewards $r_{i,t}$ to z_i and takes longer to converge for out-of-distribution instances or when the noise in the latent state is high (see Appendix E.2). For such cases we can look at the reward history and search for the latent \hat{z}_i which best explains the previous rewards and contexts, conditioned on arm parameters. This trades off exploiting the inference function f and explaining previous rewards. Our second algorithm, *full posterior greedy* (FPG), takes this approach and minimizes the full negative log-likelihood (7) to choose the best action. We can show that CPG and FPG algorithms have constant regret with respect to the horizon T for LVMs with well-specified reward models.

Theorem 3.5. *For an instance i , let $\Delta_i > 0$ such that $\forall a \neq a^* : |(\theta_{a^*} - \theta_a)^\top z_i| > \Delta_i$, let $\bar{\Delta}_i = \max_{a \neq a^*} z_i^\top (\theta_{a^*} - \theta_a)$, and assume $\forall a : \|\hat{\theta}_a\|_2 = \|\theta_a\|_2 = 1$. Then the expected regret of CPG and FPG, for an optimal model pair $(\hat{\theta}, f)$ that satisfies $\hat{\theta}^\top f(x) = \theta^\top g^{-1}(x)$, is bounded by $\text{Reg}_T \leq \frac{8K\sigma^2\bar{\Delta}_i}{\Delta_i^2}$, where σ^2 is the variance of $\eta_{i,t}$ (of $Z_{i,t}$ given Z_i).*

Table 1: LVM fitting. L layers in the MLP, $T_o = 200$ time steps per instance. Mean correlation coefficient (MCC) for \hat{z} , average R^2 for reward estimates, and % correctly identified a^* .

L	Model	MCC_Z	R_R^2	% a^*
Synthetic environment				
2	LVM	0.89	0.78	84
4	LVM	0.90	0.75	80
2	VAE	0.90	0.72	82
4	VAE	0.85	0.62	48
2	Regression	-	0.75	62
4	Regression	-	0.63	52

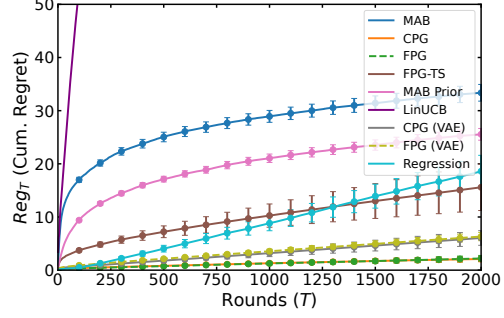


Figure 3: Cumulative regret results for ADCB comparing ILB decision-making algorithms to baselines. Error bars indicate one standard error computed with 200 seeds. The LVMs are fitted across $I = 100$ instances with $T_o = 200$ time points each with $L = 2$ layered model.

Theorem 3.5 is proven in Appendix D. Once a latent is estimated, we could either use a greedy strategy and choose the best arm under the estimated latent state, or use the posterior for the estimated reward $\hat{\mu}_i = \hat{\theta}^\top \hat{z}_i$ for *exploration*. We showcase an example of Thompson sampling on the posterior in line 9 of Algorithm 1, exploiting the fact that when the latent and reward noise is Gaussian, the estimated reward also follows a Gaussian distribution. We style the resulting algorithm as FPG-TS.

4 Experiments

Data We first create a Synthetic environment according to the structural equations in (3), with a multivariate standard Normal for U , and θ_a ’s sampled from a centralized multivariate Normal distribution, normalized to unit vectors to ensure that the optimal treatment varies with Z . For the nonlinear mixing function g , we use a randomly initialized MLP with invertible square matrices and leaky ReLU activations to ensure invertibility. We sample treatments uniformly for \mathcal{D} . At inference time, we average results over 100 problem instances with different latent states, generated from the same process. To test the sensitivity to problem parameters, we generate data with different sequence lengths T_o and with different layers L in the generating and fitting LVMs.

As a second environment, we use ADCB [21], a simulator of Alzheimer’s disease treatment. We modify the ADCB causal graph so that the latent state has categorical and continuous components, $Z_i = \{Z_i^\dagger, Z_i^{\text{cat}}\}$ where the categorical components Z_i^{cat} comprise race and sex indicators, and the continuous component Z_i^\dagger comprises the ratio of Amyloid- β ($A\beta$) plaques. The observed context ($X_{i,t}$) is a nine-dimensional mix of continuous and categorical values, generated from Z_i^{cat} as well as a noisy continuous component $Z_{i,t}^\dagger$ with $\eta_{i,t} \sim \mathcal{N}(0, 0.02)$. Eight treatments are used, with a uniformly random observational policy, and conditional rewards are further described in Appendix G.

LVM-based algorithms For our identifiable LVM, we mostly follow the network architecture and training procedure of [17] and use an MLP for the feature extractor f with hidden features as equal to dimensionality of Z_i as per Theorem 3.3. As an alternative to our identifiable LVM, we use the well-known variational autoencoder β -VAE [14], and adapt an implementation from PyOD repository [13]. We specify training details for both models in Appendix I. After training either LVM, we use the patient history to estimate the reward parameter θ . We apply decision-making algorithms CPG, FPG, and FPG-TS with both LVMs, as well as to the ground-truth inverse emission and reward models g^{-1} , θ , referred to as “oracle”. The oracle can be seen as providing the “true” model assumed known in previous latent bandit works [15].

Bandit baselines We compare to three online bandit algorithms. First, a Thompson sampling MAB [50, 43] that is oblivious to the latent state structure, initialized with Gaussian priors and

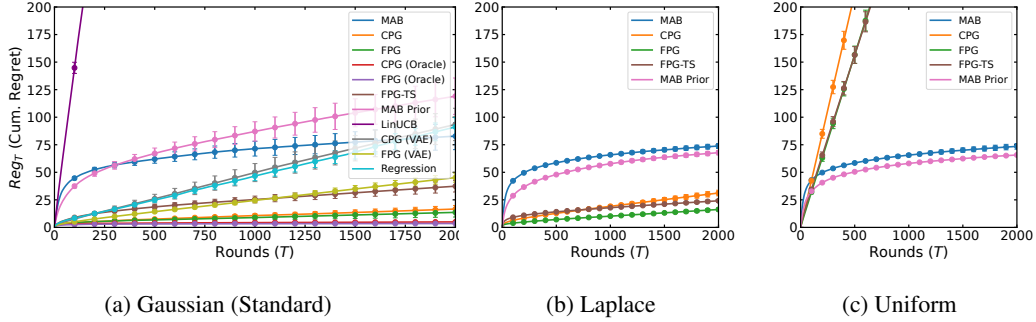


Figure 4: Cumulative regret for synthetic environment (left) comparing ILB decision-making algorithms to baselines, and comparative performance our algorithm under different exponential noise see Appendix E.6 for details). Error bars represent one standard error computed from 200 seeds. The LVMs are fitted across $I = 100$ instances with $T_i = 200$ time points each with $L = 2$ layered model.

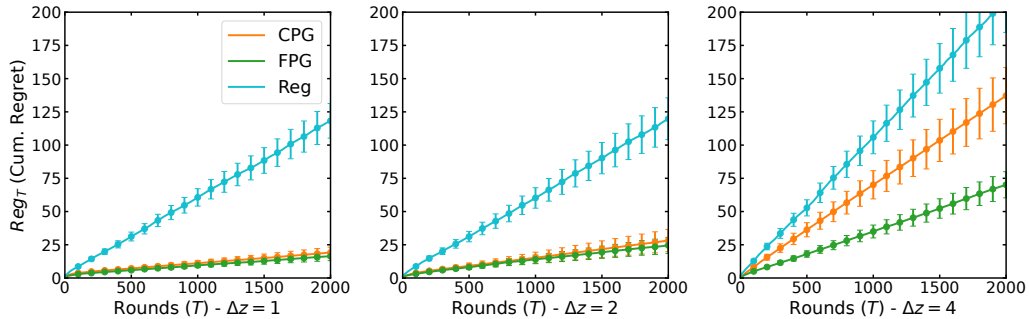


Figure 5: Cumulative regret for out-of-distribution experiments with increased Δz difference from the training distribution on the synthetic data. Error bars indicate standard error over 200 seeds.

with the ground truth variance of the reward. Second, an equivalent MAB, initialized with a one-shot prediction of rewards from the identifiable LVM, called MABPrior. Finally, we compare to a contextual upper confidence bound algorithm (LinUCB) [27].

Regression baseline We construct a Regression-based algorithm that ignores the latent structure and plays the action that maximizes an estimate of the expected reward $\mathbb{E}[R|A = a, X_1, \dots, X_t]$ given the history of contexts, similar to CPG algorithm. The contexts are sufficient adjustment sets since actions are not confounded in \mathcal{D} and the criterion is optimal given sufficiently long history. This baseline represents decision-making based on a causal effect estimator using a TARNet architecture [47]. See Appendix I for model and training details.

Evaluating LVM fit We evaluate the fits of the LVMs on the Synthetic environment using the mean correlation coefficient (MCC) used in the ICA literature [17], between the true latent states Z_i and the recovered latents \hat{z}_i , on a held-out test set of 50 patients. To assess the reward model, we report the R^2 between estimated and true potential rewards. We also look at predicted best arm and report the percentage of equaling to the optimal arm. The results are shown in Table 1. We have high MCC scores across settings, suggesting that the LVM is successful at inverting the encoding function g . Increasing the number of layers in the mixing MLP seems to make the learning and recovery tasks more difficult, which we notice especially for the VAE. We select $L = 2$ case for our bandit runs as all models have higher test R^2 in order to better analyze the pros and cons of each model. The Regression results seem comparable to other models but have a lower rate of identifying the best action in the test set. All models perform comparably well on the ADCB dataset (see Appendix H).

Results for sequential decision-making

It is possible to learn effective latent bandits The results for all decision-making algorithms on the Synthetic environment are presented as regret plots in Figure 4, and the results for ADCB in Figure 3. In both cases, offline (Regression) and hybrid (CPG, FPG, FPG-TS) algorithms converge substantially quicker than the online learners (MAB, MAB Prior, LinUCB), as expected. In Figure 4 (left), we see that the Oracle methods—latent bandits with a known, perfect model—perform the best, and that CPG and FPG (using the fitted ILB LVM) incur very small bias. This confirms that *latent bandits are feasible to learn from data, without oracle access to the LVM*. Moreover, in the Synthetic environment, CPG and FPG compare favorably to their equivalents based on the VAE LVM. This is expected since CPG, FPG use well-specified reward models, matching the parameterization of environment. In ADCB, we also see evidence that a well learned non-identifiable LVM (the VAE LVM has higher test R^2 in Table H) can still yield quick convergence, seen in CPG (VAE) in Figure 3.

Hybrid algorithms can overcome small bias in the LVM FPG-TS is based on the same LVM as CPG and FPG and samples the reward model based on the full posterior of the latent state. It converges more slowly than CPG and FPG as it explores actions to account for uncertainty in the reward model. It is however more robust to variance in the time-dependent latent variable (see Figure 8a in the Appendix). We also observed a similar behavior for FPG as it performed better than CPG for out of distribution instances in Figure 5. In Appendix E.1, we designed a set of experiments to test this behavior by adding gradual noise to X_t and thus decreasing the quality of the fitted LVM. We noted that FPG-TS gradually outperformed FPG with increasing noise while CPG was biased throughout.

Regression modeling is sensitive to limitations of observational data The regression baseline performs poorly in the Synthetic environment (Figure 4), with a substantially larger bias than the LVM-based alternative. This is consistent with the model fitting results at test time Appendix H and likely due to regression model not exploiting the structure in the data like the LVMs. On ADCB, Regression initially performs well, but quickly deteriorates. This is likely because the observational data is limited to sequences of length $T_o = 200$ but test instances have much longer horizons ($T = 2000$) and the time-series model fails to extrapolate. For the Synthetic environment, we also run out of distribution experiments in which we move the mean of U at inference time by $\Delta z = 1, \Delta z = 2, \Delta z = 4$, to the point that there is no overlap between the distributions. As seen in Figure 5, we see that CPG and FPG are more robust to shifts in the latent variable than regression (also see Appendix E.2).

About ILB algorithm We see that ILB based algorithms can be sensitive to noise in the latent state when comparing the ADCB results with different levels of latent noise (Figures 3 and 8a). Adaptive FPG and FPG-TS algorithms can overcome this bias to some extent, but are not as robust as MAB which remains unaffected. We also noticed that *Age* variable in that ADCB has unique value for each patient, which makes it trivial to predict the patient index and influences the ILB algorithm. In Appendix E.3, we show the removal of *Age* variable from the training set improves the performance.

When is online learning necessary? The MAB baseline consistently achieves low regret by the end of exploration, as expected, but converges substantially slower than all methods based on latent variable models, including FPG-TS. For the Synthetic environment the absence of bias for MAB may be sufficient for it to be preferred over the VAE and Regression baselines. Especially when the noise in the latent state is too great, such as for the uniform distribution in Figure 4, MAB becomes preferable to hybrid alternatives. We see a similar pattern on ADCB: when the latent noise increases, MAB becomes preferable over other algorithms (see Appendix E.3). This confirms the bias-variance tradeoff: a poorly fit latent variable model may find a near-optimal action quickly but suffer compared to an exploration-based algorithm in the long run.

In Appendix E.5, we show results from experiments with different numbers of actions, going from $K = 10$ to $K = 50$ that demonstrate our remark in Section 3.3 that variance in the LVM models at training time translates to bias in decision-making time.

5 Conclusion

In this work, we present the first provably identifiable latent bandit model learned from observational data for sample-efficient sequential decision-making. Our analysis proves a new identifiability result for nonlinear independent component analysis (ICA) where latent states differ only in their mean. We investigate the conditions favorable to learn such a model and test the sensitivity of our assumptions in a semi-synthetic decision-making environment. Our theoretical and empirical results demonstrate the promise of leveraging observational data in personalized decision making. For future work, we plan to generalize our identifiability assumptions, and focus on the case of where the learned LVM does not generalize well to new instances. An approach toward this goal would be to use a meta-algorithm that detects model misspecification and switches between algorithms.

References

- [1] S. Agrawal and N. Goyal. Thompson sampling for contextual bandits with linear payoffs. In *International conference on machine learning*, pages 127–135. PMLR, 2013.
- [2] S. Athey and G. W. Imbens. Machine learning methods for estimating heterogeneous causal effects. *stat*, 1050(5):1–26, 2015.
- [3] E. Bareinboim, A. Forney, and J. Pearl. Bandits with unobserved confounders: A causal approach. *Advances in Neural Information Processing Systems*, 28, 2015.
- [4] D. Bouneffouf, S. Parthasarathy, H. Samulowitz, and M. Wistub. Optimal exploitation of clustering and history information in multi-armed bandit. *arXiv preprint arXiv:1906.03979*, 2019.
- [5] L. Bui, R. Johari, and S. Mannor. Clustered bandits. *arXiv preprint arXiv:1206.4169*, 2012.
- [6] W. Chu, L. Li, L. Reyzin, and R. Schapire. Contextual bandits with linear payoff functions. In *Proceedings of the Fourteenth International Conference on Artificial Intelligence and Statistics*, pages 208–214. JMLR Workshop and Conference Proceedings, 2011.
- [7] P. Comon. Independent component analysis, a new concept? *Signal processing*, 36(3):287–314, 1994.
- [8] J. C. Gittins. Bandit processes and dynamic allocation indices. *Journal of the Royal Statistical Society Series B: Statistical Methodology*, 41(2):148–164, 1979.
- [9] M. Gutmann and A. Hyvärinen. Noise-contrastive estimation: A new estimation principle for unnormalized statistical models. In *Proceedings of the thirteenth international conference on artificial intelligence and statistics*, pages 297–304. JMLR Workshop and Conference Proceedings, 2010.
- [10] P. R. Hahn, V. Dorie, and J. S. Murray. Atlantic causal inference conference (acic) data analysis challenge 2017. *arXiv preprint arXiv:1905.09515*, 2019.
- [11] S. Håkansson, V. Lindblom, O. Gottesman, and F. D. Johansson. Learning to search efficiently for causally near-optimal treatments. *Advances in Neural Information Processing Systems*, 33:1333–1344, 2020.
- [12] S. Håkansson, V. Lindblom, O. Gottesman, and F. D. Johansson. Learning to search efficiently for causally near-optimal treatments. *Advances in Neural Information Processing Systems*, 33:1333–1344, 2020.
- [13] S. Han, X. Hu, H. Huang, M. Jiang, and Y. Zhao. Adbench: Anomaly detection benchmark. *Advances in Neural Information Processing Systems*, 35:32142–32159, 2022.
- [14] I. Higgins, L. Matthey, A. Pal, C. P. Burgess, X. Glorot, M. M. Botvinick, S. Mohamed, and A. Lerchner. beta-vae: Learning basic visual concepts with a constrained variational framework. *ICLR (Poster)*, 3, 2017.
- [15] J. Hong, B. Kveton, M. Zaheer, Y. Chow, A. Ahmed, and C. Boutilier. Latent bandits revisited. *Advances in Neural Information Processing Systems*, 33:13423–13433, 2020.
- [16] E. K. Huch, J. Shi, M. R. Abbott, J. R. Golbus, A. Moreno, and W. H. Dempsey. RoME: A robust mixed-effects bandit algorithm for optimizing mobile health interventions. In *The Thirty-eighth Annual Conference on Neural Information Processing Systems*, 2024.
- [17] A. Hyvarinen and H. Morioka. Unsupervised feature extraction by time-contrastive learning and nonlinear ica. *Advances in neural information processing systems*, 29, 2016.
- [18] A. Hyvarinen, H. Sasaki, and R. Turner. Nonlinear ica using auxiliary variables and generalized contrastive learning. In *The 22nd International Conference on Artificial Intelligence and Statistics*, pages 859–868. PMLR, 2019.

- [19] I. Khemakhem, D. Kingma, R. Monti, and A. Hyvarinen. Variational autoencoders and nonlinear ica: A unifying framework. In *International Conference on Artificial Intelligence and Statistics*, pages 2207–2217. PMLR, 2020.
- [20] N. M. Kinyanjui, E. Carlsson, and F. D. Johansson. Fast treatment personalization with latent bandits in fixed-confidence pure exploration. *Transactions on Machine Learning Research*, 2023. Expert Certification.
- [21] N. M. Kinyanjui and F. D. Johansson. Adcb: An alzheimer’s disease simulator for benchmarking observational estimators of causal effects. In *Conference on Health, Inference, and Learning*, pages 103–118. PMLR, 2022.
- [22] T. Kocák, R. Munos, B. Kveton, S. Agrawal, and M. Valko. Spectral bandits. *Journal of Machine Learning Research*, 21(218):1–44, 2020.
- [23] S. R. Künnel, J. S. Sekhon, P. J. Bickel, and B. Yu. Metalearners for estimating heterogeneous treatment effects using machine learning. *Proceedings of the national academy of sciences*, 116(10):4156–4165, 2019.
- [24] F. Lattimore, T. Lattimore, and M. D. Reid. Causal bandits: Learning good interventions via causal inference. *Advances in neural information processing systems*, 29, 2016.
- [25] T. Lattimore and C. Szepesvári. *Bandit algorithms*. Cambridge University Press, 2020.
- [26] S. Lee and E. Bareinboim. Structural causal bandits: Where to intervene? *Advances in neural information processing systems*, 31, 2018.
- [27] L. Li, W. Chu, J. Langford, and R. E. Schapire. A contextual-bandit approach to personalized news article recommendation. In *Proceedings of the 19th international conference on World wide web*, pages 661–670, 2010.
- [28] C. Louizos, U. Shalit, J. M. Mooij, D. Sontag, R. Zemel, and M. Welling. Causal effect inference with deep latent-variable models. *Advances in neural information processing systems*, 30, 2017.
- [29] Z. Lu, Y. Cheng, M. Zhong, G. Stoian, Y. Yuan, and G. Wang. Causal effect estimation using variational information bottleneck. In *International Conference on Web Information Systems and Applications*, pages 288–296. Springer, 2022.
- [30] O.-A. Maillard and S. Mannor. Latent bandits. In *International Conference on Machine Learning*, pages 136–144. PMLR, 2014.
- [31] O.-A. Maillard and S. Mannor. Latent bandits. In *International Conference on Machine Learning*, pages 136–144. PMLR, 2014.
- [32] S. A. Murphy, L. M. Collins, and A. J. Rush. Customizing treatment to the patient: Adaptive treatment strategies, 2007.
- [33] B. Oetomo, R. M. Perera, R. Borovica-Gajic, and B. I. Rubinstein. Cutting to the chase with warm-start contextual bandits. *Knowledge and Information Systems*, 65(9):3533–3565, 2023.
- [34] B. Oetomo, R. M. Perera, R. Borovica-Gajic, and B. I. Rubinstein. Warm-starting contextual bandits under latent reward scaling. *ICDM*, 2024.
- [35] J. Pearl. *Causality*. Cambridge university press, 2009.
- [36] N. Radcliffe. Using control groups to target on predicted lift: Building and assessing uplift model. *Direct Marketing Analytics Journal*, pages 14–21, 2007.
- [37] V. Rakesh, R. Guo, R. Moraffah, N. Agarwal, and H. Liu. Linked causal variational autoencoder for inferring paired spillover effects. In *Proceedings of the 27th ACM International Conference on Information and Knowledge Management*, pages 1679–1682, 2018.
- [38] D. Rezende and S. Mohamed. Variational inference with normalizing flows. In *International conference on machine learning*, pages 1530–1538. PMLR, 2015.

- [39] H. Robbins. Some aspects of the sequential design of experiments. *Bulletin of the American Mathematical Society*, 58(5):527–535, 1952.
- [40] P. R. Rosenbaum, P. Rosenbaum, and Briskman. *Design of observational studies*, volume 10. Springer, 2010.
- [41] D. B. Rubin. Causal inference using potential outcomes: Design, modeling, decisions. *Journal of the American Statistical Association*, 100(469):322–331, 2005.
- [42] A. Russo, A. M. Metelli, and M. Restelli. Switching latent bandits. *Transactions on Machine Learning Research*, 2024.
- [43] D. J. Russo, B. Van Roy, A. Kazerouni, I. Osband, Z. Wen, et al. A tutorial on thompson sampling. *Foundations and Trends® in Machine Learning*, 11(1):1–96, 2018.
- [44] B. Schölkopf, F. Locatello, S. Bauer, N. R. Ke, N. Kalchbrenner, A. Goyal, and Y. Bengio. Toward causal representation learning. *Proceedings of the IEEE*, 109(5):612–634, 2021.
- [45] B. Schölkopf, F. Locatello, S. Bauer, N. R. Ke, N. Kalchbrenner, A. Goyal, and Y. Bengio. Toward causal representation learning. *Proceedings of the IEEE*, 109(5):612–634, 2021.
- [46] R. Sen, K. Shanmugam, M. Kocaoglu, A. Dimakis, and S. Shakkottai. Contextual bandits with latent confounders: An nmf approach. In *Artificial Intelligence and Statistics*, pages 518–527. PMLR, 2017.
- [47] U. Shalit, F. D. Johansson, and D. Sontag. Estimating individual treatment effect: generalization bounds and algorithms. In *International conference on machine learning*, pages 3076–3085. PMLR, 2017.
- [48] J. A. Singh, K. G. Saag, S. L. Bridges Jr, E. A. Akl, R. R. Bannuru, M. C. Sullivan, E. Vaysbrot, C. McNaughton, M. Osani, R. H. Shmerling, et al. 2015 american college of rheumatology guideline for the treatment of rheumatoid arthritis. *Arthritis & rheumatology*, 68(1):1–26, 2016.
- [49] A. A. Tahami Monfared, N. N. Phan, I. Pearson, J. Mauskopf, M. Cho, Q. Zhang, and H. Hampel. A systematic review of clinical practice guidelines for alzheimer’s disease and strategies for future advancements. *Neurology and therapy*, 12(4):1257–1284, 2023.
- [50] W. R. Thompson. On the likelihood that one unknown probability exceeds another in view of the evidence of two samples. *Biometrika*, 25(3/4):285–294, 1933.
- [51] R. Vershynin. *High-dimensional probability: An introduction with applications in data science*, volume 47. Cambridge university press, 2018.
- [52] Y. Wang and M. I. Jordan. Desiderata for representation learning: A causal perspective. *arXiv preprint arXiv:2109.03795*, 2021.
- [53] L. Yao, Z. Chu, S. Li, Y. Li, J. Gao, and A. Zhang. A survey on causal inference. *ACM Transactions on Knowledge Discovery from Data (TKDD)*, 15(5):1–46, 2021.
- [54] C. Zhang, A. Agarwal, H. Daumé III, J. Langford, and S. N. Negahban. Warm-starting contextual bandits: Robustly combining supervised and bandit feedback. *arXiv preprint arXiv:1901.00301*, 2019.
- [55] K. Zhong, F. Xiao, Y. Ren, Y. Liang, W. Yao, X. Yang, and L. Cen. Descn: Deep entire space cross networks for individual treatment effect estimation. In *Proceedings of the 28th ACM SIGKDD Conference on Knowledge Discovery and Data Mining*, pages 4612–4620, 2022.
- [56] L. Zhou. A survey on contextual multi-armed bandits. *arXiv preprint arXiv:1508.03326*, 2015.

Appendix

A Notation

Table 2: Notation. Indices that indicate problem instances i and time points t are dropped when clear from context (e.g., when stated to be fixed in text or in i.i.d. distributions over multiple instances)

Random variables	
Z_i	Latent state for problem instance i
$Z_{i,t}$	Time-varying (noisy) latent state for problem instance i at time t
U	Population distribution of latents Z_i
$X_{i,t}$	Context for instance i at time t
$A_{i,t}$	Action for instance i at time t
$R_{i,t}$	Reward for instance i at time t
$\eta_{i,t}$	Noise variable for $Z_{i,t}$
$\epsilon_{i,t}$	Noise variable for $R_{i,t}$
$H_{i,t}$	Stochastic history of past contexts, actions and rewards up to time t for instance i
Reg_T	Expected cumulative regret
Observations and constants	
\mathcal{D}	Observational data consisting of logs of treatments for multiple individuals
z_i	Latent state for problem instance i
$z_{i,t}$	Time-varying (noisy) latent state for problem instance i at time t
$x_{i,t}$	Context for instance i at time t
$a_{i,t}$	Action for instance i at time t
$r_{i,t}$	Reward for instance i at time t
T_i	Number of observations for instance i in the dataset \mathcal{D}
I	Total number of patients included in the dataset \mathcal{D}
n	Dimensions of the latent state
d	Dimensions of the context
\mathcal{A}	Set of all action instances
K	Total number of actions (i.e. $ \mathcal{A} $)
$\mu_a(z)$	Expected reward for action a conditioned on latent state Z
σ^2	Variance associated with the latent noise variable $\eta_{i,t}$
μ_i^*	Optimal reward for instance i
a_i^*	Optimal action for instance i
M	Matrix of all instance means z_i
B, b	Affine transformation constants for the identification of latent state
Functions	
g	Non-linear transformation mapping the latent state to context variable
f	Feature extractor for the learned representation from context to latent variables
W, b	Weight and biases for the multinomial linear regression
θ_a	Parameter vector for action a

B Identifiability of the latent variable model

Hyvärinen and Morioka [17] give an argument for recovering the conditional probability of the patient/instance indicator (in their case, “segment”), stated here as Lemma B.1.

Lemma B.1 ([17]). *For the classifier given in equation (4), in the limit of per-instance infinite data the optimal feature extractor f^* given by*

$$f^*, q^* = \arg \max_{f, q} \lim_{T_i \rightarrow \infty} \sum_{i=1}^I \sum_{t=1}^{T_i} \log \left[\frac{e^{q_i(f(x_{i,t}))}}{1 + \sum_{j=2}^I e^{q_j(f(x_{i,t}))}} \right] \quad (8)$$

would converge to the true posterior $p(C|X)$:

$$p(C = c | X = x) = \frac{p_c(X = x) p(C = c)}{\sum_{j=1}^I p_j(X = x) p(C = j)}, \quad (9)$$

where C is the (instance) class label of X , $p_c(X = x) = p(X = x | C = c)$ is the conditional distribution of the context for instance class c , and $p(C = c)$ are prior distributions for each instance. Then we have for $f^*(x)$:

$$W_c^T f^*(x) + b_c = \log p_c(x) - \log p_1(x) + \rho_c, \quad (10)$$

where $\rho_c = \frac{p(C=c)}{p(C=1)}$ relates to the length (number of samples) of each instance sequence.

B.1 Proof of Theorem 3.3

Theorem 3.3 (Restated) (Identifiability of Structural Equations 3). *Under Assumptions 3.1–3.2, in the limit of infinite per-instance data, the outputs of an optimal feature extractor f^* , according to (5), are equal to instance mean distribution up to an invertible affine transformation. In other words,*

$$B f^*(x) + b = g^{-1}(x) \quad (11)$$

for some constant invertible matrix $B \in \mathbb{R}^{d \times d}$, a constant vector $b \in \mathbb{R}^d$.

Proof. According to Assumption 3.1 the conditional distribution of each $Z_{i,t}$ will be normally distributed around the true mean Z_i , with mean z_i and variance σ^2 . For each time point $z_{i,\cdot}$ the log-pdf of the product distribution can be written as:

$$\log \mathbb{P}(Z_{i,\cdot} = \zeta) = \log p_i(\zeta) = \sum_{j=1}^n \frac{(\zeta_j - z_{i,j})^2}{\sigma^2}, \quad (12)$$

where we use j to indicate the dimension. Using change of variables for the data generating distribution g^{-1} we have:

$$\log p_i(x) = \sum_{j=1}^n \frac{(g_j^{-1}(x) - z_{i,j})^2}{\sigma^2} + \log |\det \mathbf{J} g^{-1}(x)|, \quad (13)$$

where \mathbf{J} is the Jacobian matrix. We look at the instance with index $i = 1$, following from line (13), we have:

$$\log p_1(x) = \sum_{j=1}^n \frac{(g_j^{-1}(x) - z_{1,j})^2}{\sigma^2} + \log |\det \mathbf{J} g^{-1}(x)| \quad (14)$$

Using (14) for the $\log p_1$ term in Lemma B.1:

$$\log p_i(x) = \sum_{j=1}^n \left[W_{i,j} f_j^*(x) + \frac{(g_j^{-1}(x) - z_{1,j})^2}{\sigma^2} \right] + \log |\det \mathbf{J} g^{-1}(x)| + b_i - \rho_i \quad (15)$$

Finally, taking (15) and (13) equal for arbitrary i , the Jacobian terms cancel:

$$\sum_{j=1}^n \frac{(g_j^{-1}(x) - z_{i,j})^2 - (g_j^{-1}(x) - z_{1,j})^2}{\sigma^2} = \sum_{j=1}^n W_{i,j} f_j^*(x) + b_i - \rho_i \quad (16)$$

Simplifying (16) for $\mathbf{b}_i = b_i - c_i - \frac{z_{i,j}^2 - z_{1,j}^2}{\sigma^2}$, $\mathbf{B}_{i,j} = \frac{-2g_j^{-1}(x)}{\sigma^2}$, and $\tilde{z}_{i,j} = z_{i,j} - z_{1,j}$

$$\sum_{j=1}^n \mathbf{B}_{i,j} \tilde{z}_{i,j} = \sum_{j=1}^n W_{i,j} f_j^*(x) + \mathbf{b}_i \quad (17)$$

which identifies the patient mean z_i up to an affine transformation. Observe that the identification requires patient means z_i to be sufficiently different, in particular there should be at least n linearly independent components as per assumption (b). \square

B.2 Generalization to other exponential-family distributions

Previous works on non-linear ICA [17, 18] gave identifiability guarantees for exponential family of the form which we express in our notation as

$$p(Z_{i,t} | Z_i = z_i) = \frac{Q(z_i)}{M(z_i)} \exp \left[\sum_{j=1}^n T_{ij}(z_i) \lambda_{ij} \right], \quad (18)$$

where T sufficient statistic, $\lambda_{i,j}$, $Q(z_i)$, and normalizing constant M scalar-valued functions. The distributions. Notably the parametric form in (18) is a limited form of the exponential family as it assumes a mean-zero distribution. However, in our case when η_t comes from such a family. $Z_{i,t} = Z_i + \eta_{i,t}$ has the mean term Z_i . Here we give an identifiability result for a different parameterization of a subset of exponential family distributions, adjusted to our setting in Corollary B.2. We also give experimental results for well-known exponential family distributions in Appendix E.6.

Corollary B.2. *The identification result in Theorem 3.3 can be generalized for $\eta_{i,t}$ coming from an exponential product distribution of the form: $\eta_{i,t}(\zeta) \sim \prod \frac{1}{M} \exp[\eta T(\zeta) - z_i]$, where $T(\cdot)$ is the sufficient statistic and η is a scalar, and M is the normalizing constant.*

Proof. The proof follows the same steps as Theorem 3.3 and gives a parametric identifiability of the latent state. In particular, the log-pdf can be written as a product distribution.

$$\log \mathbb{P}(Z_{i,\cdot} = \zeta) = \log p_i(\zeta) = \sum_{j=1}^n \eta T(\zeta_j) - z_{i,j} - \log(M) \quad (19)$$

where we use j to indicate the dimension. Using change of variables for the data generating distribution g^{-1} we have:

$$\log p_i(x) = \sum_{j=1}^n \eta T(g_j^{-1}(x)) - z_{i,j} + \log |\det \mathbf{J} g^{-1}(x)| - \log(M), \quad (20)$$

Following the steps in Theorem 3.3, we have

$$\log p_i(x) = \sum_{j=1}^n [W_{i,j} f_j(x) + T(g_j^{-1}(x)) - z_{1,j}] + \log |\det \mathbf{J} g^{-1}(x)| - \log(M) + b_i - \rho_i \quad (21)$$

Equation two terms we get cancellation of the $\log(M)$ and Jacobian terms:

$$\sum_{j=1}^n \eta T(g_j^{-1}(x)) - z_{i,j} - \eta T(g_j^{-1}(x)) + z_{1,j} = \sum_{j=1}^n [W_{i,j} f_j(x)] + b_i - \rho_i \quad (22)$$

and simplifying for $\tilde{z}_{i,j} = z_{1,j} - z_{i,j}$ and $\tilde{b} = b_i - \rho_i$ we get

$$\sum_{j=1}^n \tilde{z}_{i,j} = \sum_{j=1}^n W_{i,j} f_j(x) + \tilde{b}, \quad (23)$$

which identifies the patient mean z_i up to an affine transformation. □

C Identifiability of decision-making criteria

Theorem 3.4 (Restated). Assume that reward means are linear, $\mu_a(z) = \theta_a^\top z$, and fix a problem instance i . Then, under the conditions of Assumption 3.1, the state-conditional expected reward $\mathbb{E}[R_{i,t} \mid Z_i = z, \text{do}(A_{i,t} = a)]$ of an intervention a is identifiable from the observational distribution of problem instances $p(H_T)$ by the OLS regression estimand applied to observed rewards and latent states inferred by an optimal feature extractor f in the sense of Theorem 3.3.

Proof. First, let's begin with the identification of $\mathbb{E}[R_{i,t} \mid Z_i, \text{do}(a)]$ under the assumption that Z could be observed directly and generalize this later. Under Assumption 3.1, the reward is stationary conditioned on Z and the action.

Step 1: Causal identifiability of the reward model

Assume that the system of variables $Z_i, Z_{i,t}, X_{i,t}, A_{i,t}, R_{i,t}$ for all instances i and time points t obey the structural causal model of Assumption 3.1. Then, for a fixed instance i , at all time points t , the causal graph in our structural causal model satisfies the backdoor criterion [35] for the effect on $R_{i,t}$ of an intervention on $A_{i,t}$ by conditioning on Z . In other words, Z blocks all backdoor paths from $R_{i,t}$ ending in $A_{i,t}$. Therefore,

$$\mathbb{E}[R_{i,t} \mid Z_i = z, \text{do}(A_{i,t} = a)] = \mathbb{E}[R_{i,t} \mid Z_i = z, A_{i,t} = a].$$

Moreover, since $R_{i,t}$ is stationary in both time and across problem instances conditioned on a and z ,

$$\mathbb{E}[R_{i,t} \mid Z_i = z, A_{i,t} = a] = \mathbb{E}[R \mid Z = z, A = a].$$

Hence, the expected reward following an intervention a is identifiable from the observational distribution $p(X_1, A_1, R_1, \dots, X_T, A_T, R_T)$ ¹ under the data-generating process of Assumption 3.1.

Step 2: Identification without observing Z

From Step 1, it is clear that we can identify the expected reward of an action conditioned on the fixed latent state Z_i of an individual. However, since the latent state is unobserved, we must infer it from observed variables for the reward to be identifiable. First, assume that we have access to the oracle LVM (g^{-1}, θ) that generated the observational data and the current problem instance. We will generalize this to invariance under an affine transform later.

For any time step t and instance i , it holds under Assumption 3.1 that

$$Z_{i,t} = g^{-1}(X_{i,t}) \quad \text{and} \quad \mathbb{E}[R_{i,t} \mid Z_i, A_{i,t} = a] = \theta_a^\top Z_i.$$

Moreover, since $\forall t : Z_{i,t} \sim \mathcal{N}(Z_i, \sigma^2 \mathbb{I})$ by assumption, $\mathbb{E}[Z_{i,t} \mid Z_i] = Z_i$. Since $Z_{i,t}$ is stationary in time given Z_i , we may drop the time index and view this expectation as an integral in time. Due to the invertibility of g , we have

$$\mathbb{E}[R_{i,t} \mid Z_i, A_{i,t} = a] = \mathbb{E}[R_{i,t} \mid \mathbb{E}[g^{-1}(X_{i,\cdot})], A_{i,t} = a] = \theta_a^\top \mathbb{E}[g^{-1}(X_{i,\cdot})].$$

From Theorem 3.3, we know that g^{-1} can be identified up to an affine transformation. We'll deal with this invariance next.

Step 3: Invariance to affine transform

Since Z_i is not observed directly, we rely on the learned representation $\hat{Z}_{i,t} = f(X_{i,t})$. Dropping the instance index i , by Theorem 3.3, a feature extractor f may be partially identified from the observational distribution such that $\hat{z}_t = f(x_t)$ satisfies:

$$z_t = B\hat{z}_t + b,$$

where B is an invertible matrix, and b is a constant vector. Substituting Z in terms of \hat{Z} into the reward model for a fixed instance i , following action $A_t = a$ and dropping the time index for convenience,

$$R = \theta_a^\top Z + \epsilon_a = \theta_a^\top \mathbb{E}[Z_t] + \epsilon_a = \theta_a^\top \mathbb{E}[B\hat{z}_t + b] + \epsilon_a = \theta_a^\top (B\mathbb{E}[\hat{z}_t] + b) + \epsilon_a.$$

¹Here, we suppress the instance index i since instances are assumed to be i.i.d.

Introducing transformed coefficients: $\tilde{\theta}_a = B\theta_a$ and $\tilde{b}_a = \theta_a^\top b$, we find that

$$R = \tilde{\theta}_a^\top \mathbb{E}[\hat{z}_{(\cdot)}] + \tilde{b}_a + \epsilon_a.$$

Thus, the expected reward depends linearly on $\hat{z} = \mathbb{E}[\hat{z}_{(\cdot)}]$, with transformed coefficients,

$$\mathbb{E}[R \mid Z = z, \mathbf{do}(A = a)] = \tilde{\theta}_a^\top \hat{z} + \tilde{b}_a.$$

Now, consider a dataset generated by inferring Z from the observational distribution $p(H_T)$ with samples $(\hat{z}_i, a_{i,t}, r_{i,t})$ for a range of instances i and time points t , where $\hat{z}_i = \mathbb{E}[f(x_{i,\cdot})]$. The ordinary least squares (OLS) estimator applied separately to samples sets $\{(\hat{z}_i, r_{i,t})\}$ for each action will return parameters $(\tilde{\theta}_a, \tilde{b}_a)$ in expectation, since OLS is unbiased. Hence, $\mathbb{E}[R \mid Z, A = a]$ is identifiable from the observational distribution. \square

Remark on Theorem 3.4

By the previous section, affine transformations of \hat{Z} do not affect the ordering of $\hat{\theta}_A^\top \hat{Z}$ as long as reward parameters $\hat{\theta}_a$ are fit to this estimate. More explicitly, if we consider two actions a_1 and a_2 , then for any fixed \hat{z} ,

$$\theta_{a_1}^\top z > \theta_{a_2}^\top z \iff \tilde{\theta}_{a_1}^\top \hat{z} + \tilde{b}_{a_1} > \tilde{\theta}_{a_2}^\top \hat{z} + \tilde{b}_{a_2}.$$

This is because B is invertible, so it induces a one-to-one transformation between Z , and \hat{z} and does not affect the relative ordering of actions. Neither does the additive term \tilde{b}_A affect the relative ordering of actions. Consequently,

$$a^*(z) = \arg \max_a \theta_A^\top z = \arg \max_a [(\theta_A^\top A)\hat{z} + \theta_A^\top b]. \quad (24)$$

Therefore, the optimal policy satisfies:

$$a^*(z) = a^*(B\hat{z} + b) = a^*(\hat{z}).$$

D CPG and FPG has constant regret

In this section, we go over the proof of Theorem 3.5. We assume that we have access to an optimal feature extractor f in the sense of Theorem 3.3 and an OLS estimate of the rewards $\hat{\theta}$ as in Theorem 3.4. From these two we develop a notion of optimal model pair $(\hat{\theta}, f)$ where $\hat{\theta}^\top f(x) = \theta^\top g^{-1}(x)$ for $x \in \mathbb{R}^d$. More explicitly,

$$\theta^\top g^{-1}(x) = \theta^\top (Bf(x) + b) = \theta^\top Bf(x) + \theta^\top b = \hat{\theta}^\top f(x), \quad (25)$$

where $\theta^\top B$ is the coefficient and $\theta^\top b$ is the intercept term for $\hat{\theta}$. First, we show that FPG estimate is unbiased and distributed Gaussian around $f(g(z_i))$, the fixed affine transform around the true mean, z_i .

Lemma D.1 (Estimator for FPG). *For an instance i and under an optimal model pair $(\hat{\theta}, f)$, in the sense of Theorem 3.5, the estimate \hat{z}_i for FPG as given in equation (7) in Algorithm 1, for any time step t , is distributed Gaussian around $f(g(z_i))$, the fixed affine transform around the true mean, z_i .*

Proof. The FPG algorithm decides on \hat{z}_i for each time point by t using the convex optimization problem (7) applied to the current history and context, h_t, x_t , in Algorithm 1. We write the corresponding loss function for the optimization problem as $\ell(z)$:

$$\ell(z) = \sum_{t'=1}^t (r_{t'} - \hat{\theta}_{a_{t'}}^\top z)^2 + \|z - \bar{z}_t\|^2$$

where we used the short hand $\bar{z}_t = \frac{1}{t} \sum_{t'=1}^t f(x_{t'})$ for the LVM mean estimate. Taking the gradient with respect to z :

$$-\frac{1}{2}\nabla_z \ell = \sum_{t'=1}^t (r_{t'} - \hat{\theta}_{a_{t'}}^\top z)^\top \hat{\theta}_{a_{t'}} + (\bar{z}_t - z)$$

Rearranging terms can be rewritten as:

$$= \sum_{t'=1}^t (r_{t'} \hat{\theta}_{a_{t'}} + \bar{z}_t)^\top - \hat{\theta}_{a_{t'}} \hat{\theta}_{a_{t'}}^\top z - z.$$

Taking $-\frac{1}{2}\nabla_z \ell = 0$ implies:

$$z = \sum_{t'} (\hat{\theta}_{a_{t'}} \hat{\theta}_{a_{t'}}^\top + \mathbb{I})^{-1} \sum_{t'} (r_{t'} \hat{\theta}_{a_{t'}} + \bar{z}_t)^\top, \quad (26)$$

which gives us a closed form for \hat{z}_i that minimizes $\ell(z)$. Next, we wish to show that \hat{z}_i is normally distributed around $f(g(z_i))$. By the affine identifiability presented in Theorem 3.3, we have :

$$f(x_t) = f(g(z_i + \eta_t)) = B^{-1}(g^{-1}(g(z_i + \eta_t)) - b) = f(g(z_i)) + \tilde{\eta}_t \quad (27)$$

$$r_t = \theta_a^\top z + \epsilon_{a_t} = \hat{\theta}_{a_t}^\top f(g(z_i)) + \tilde{b}_{a_t} + \epsilon_{a_t} \quad (28)$$

where z_i is the true instance mean. $\tilde{\eta}_t = B^{-1}\eta_t - b$, and $\tilde{b}_a = \theta_a^\top b$ results from affine identifiability. We discuss in the Remark on Appendix C the effect of affine identifiability on the rewards. In practice, for an optimal model pair the fitted OLS estimator $\hat{\theta}$ will have an intercept term $\hat{\theta}_0 = \tilde{b}_a$ as given by Equation (25). However, for FPG we treat θ as fixed and fit a \hat{z}_i instead, using the bilinearity of the reward. With a fixed theta, the reward with respect to z is $r_t = \theta_a^\top z + \theta_0$, which would leave the term θ_0 without an intercept fit for z . Therefore, we would need to fit an intercept term for the FPG estimate \hat{z}_i to remove any bias, $r_t = \theta_a^\top z + \theta_0^\top z_{(0)}$. We denote the bias term as $z_{(0)}$ and separate Equation (26) into two parts:

$$z + z_{(0)} = \sum_{t'} (\hat{\theta}_{a_{t'}} \hat{\theta}_{a_{t'}}^\top + \mathbb{I})^{-1} \sum_{t'} \left(f(g(z_i)) \hat{\theta}_{a_{t'}} \hat{\theta}_{a_{t'}}^\top + f(g(z_i)) \right)^\top \quad (29)$$

$$+ \sum_{t'} (\hat{\theta}_{a_{t'}} \hat{\theta}_{a_{t'}}^\top + \mathbb{I})^{-1} \sum_{t'} (\epsilon_{a_{t'}} + \tilde{b}_{a_t}) \hat{\theta}_{a_{t'}} \hat{\theta}_{a_{t'}}^\top + \tilde{\eta}_t. \quad (30)$$

As η_t and ϵ_{a_t} are Gaussian the term (30) is stochastic. As there is no dependence on f , we can absorb the mean parameter in to the intercept term $z_{(0)}$ and treat it as mean-zero Gaussian. The term (29) is deterministic, and is given by:

$$\begin{aligned} &= \sum_{t'} (\hat{\theta}_{a_{t'}} \hat{\theta}_{a_{t'}}^\top + \mathbb{I})^{-1} \sum_{t'} (f(g(z_i)) \hat{\theta}_{a_{t'}} \hat{\theta}_{a_{t'}}^\top + f(g(z_i)))^\top \\ &= \sum_{t'} (\hat{\theta}_{a_{t'}} \hat{\theta}_{a_{t'}}^\top + \mathbb{I})^{-1} f(g(z_i)) \sum_{t'} (\hat{\theta}_{a_{t'}} \hat{\theta}_{a_{t'}}^\top + \mathbb{I}) \\ &= f(g(z_i)). \end{aligned}$$

This concludes the proof that the estimate for FPG is Gaussian around $f(g(z_i))$, the fixed affine transform around the true mean, z_i . \square

Now, we're ready to show our result on cumulative regret of CPG and FPG algorithms. It follows from standard concentration results for sub-Gaussian random variables, see Theorem D.2.

Theorem 3.5 (Restated). *For a given instance i , let $\Delta_i > 0$ such that $|(\theta_{a^*} - \theta_a)^\top z_i| > \Delta, \forall a \neq a^*$, let $\bar{\Delta}_i = \max_{a \neq a^*} z_i^\top (\theta_{a^*} - \theta_a)$, and assume $\|\hat{\theta}_a\|_2 = \|\theta_a\|_2 = 1, \forall a$. Then the expected regret of CPG, for the optimal model pair $(\hat{\theta}, f)$ that satisfy $\hat{\theta}^\top f(x) = \theta^\top g^{-1}(x)$, is bounded by*

$$\text{Reg}_T \leq \frac{8K\sigma^2\bar{\Delta}_i}{\Delta_i^2}.$$

Proof. We first start with the observation that

$$\left| (\theta_{a^*} - \theta_a)^\top z_i \right| = \left| (\hat{\theta}_{a^*} - \hat{\theta}_a)^\top f(g(z_i)) \right|,$$

follows from our assumptions. CPG will play a sub-optimal arm a if $\hat{\theta}_a^\top \hat{z}_{i,t} \geq \hat{\theta}_{a^*}^\top \hat{z}_{i,t}$ where

$$\hat{z}_t := \frac{1}{t} \sum_{t'=1}^t f(x_{i,t'}),$$

for CPG and given by (26) in proof of Lemma D.1 for FPG.

Hence, if for all arms we have

$$\left| \hat{\theta}_a^\top (\hat{z}_t - f(g(z_i))) \right| \leq \frac{\Delta_i}{2}$$

CPG and FPG will play the optimal arm. We use the fact that CPG and FPG distributed Gaussian around $f(g(z_i))$. We give the bound for CPG, and FPG follows from similar arguments. Note that we have:

$$\left| \hat{\theta}_a^\top (\hat{z}_t - f(g(z_i))) \right| = \frac{1}{t} \left| \hat{\theta}_a^\top \sum_{t'=1}^t \eta_{t'} \right|$$

since each latent $z_{i,t'} = z_i + \eta_{i,t'}$ where each element in $\eta_{t'}$ is $\mathcal{N}(0, \sigma^2)$.

Hence, using the union bound,

$$\text{Reg}_T \leq \bar{\Delta}_i \sum_a \sum_{t=1}^T P \left(\left| \hat{\theta}_a^\top \sum_{t'=1}^t \eta_{t'} \right| \geq \frac{\Delta_i}{2} \right)$$

where $\bar{\Delta} = \max_{a \neq a^*} z_i^\top (\theta_{a^*} - \theta_a)$.

We now apply Theorem D.2 with $w = \theta_a$ which yields

$$P \left(\left| \hat{\theta}_a^\top \sum_{t'=1}^t \eta_{t'} \right| \geq \frac{\Delta_i}{2} \right) \leq 2 \exp \left[-\frac{t\Delta_i^2}{4\sigma^2} \right]$$

since $\|\hat{\theta}_a\| = 1$. Putting it together yields

$$\text{Reg}_T \leq K\bar{\Delta}_i \sum_{t=1}^{\infty} 2 \exp \left[-\frac{t\Delta_i^2}{4\sigma^2} \right] = 2K\bar{\Delta}_i \left(\exp \left[\frac{\Delta_i^2}{4\sigma^2} \right] - 1 \right)^{-1}.$$

Now using the fact that

$$\frac{1}{e^x - 1} \leq \frac{1}{x}$$

yields

$$\text{Reg}_T \leq \frac{8K\sigma^2\bar{\Delta}_i}{\Delta_i^2} \tag{31}$$

□

Theorem D.2 (General Hoeffding's Inequality [51]). *Let X_1, \dots, X_d be independent, zero-mean, sub-Gaussian random variables and let $w \in \mathbb{R}^d$. Then for every $\gamma > 0$*

$$P \left(\left| \sum_{i=1}^d X_i w_i \right| \geq \gamma \right) \leq 2 \exp \left[-\frac{\gamma^2}{Q^2 \|w\|_2^2} \right]$$

with Q^2 equal to the maximum variance of any of the X_i 's.

Synthetic Data			
σ	Model	R_R^2	% a^*
0.25	LVM	0.73	76
0.25	VAE	0.73	80
0.25	Reg.	0.72	69
0.5	LVM	0.71	75
0.5	VAE	0.72	74
0.5	Reg.	0.70	61
1	LVM	0.70	68
1	VAE	0.73	77
1	Reg.	0.65	56

Table 3: The LVM fitting results for increasing noise in X_t . We fit the models for $L = 2$ and $T_o = 200$, the results are averaged over 10 seeds.

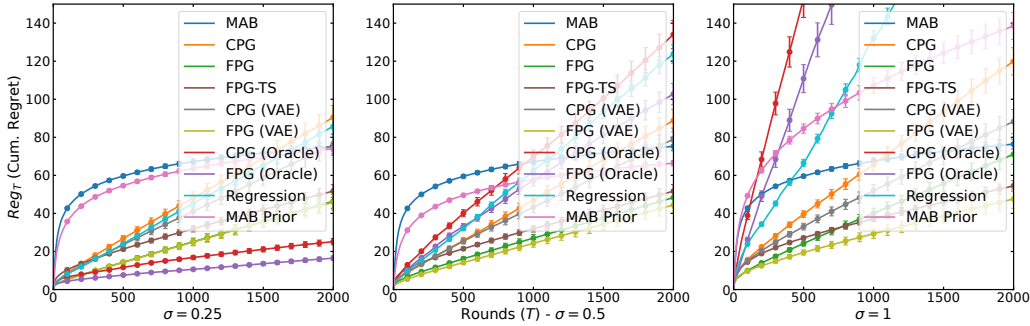


Figure 6: Expected cumulative regret ILB and baseline algorithms for different levels of standard deviation $\sigma = 0.25, 0.5$, and 1 Gaussian noise in the context X_t . The error bars show standard error calculated across 1000 seeds.

E Additional Experiments

E.1 Ablation for identifiability

In order to test the adaptability of CPG and FPG algorithms to where our assumptions breakdown. We prepared a set of experiments where we gradually added Gaussian noise to the X_t in the synthetic setting. Adding such noise breaks down our identifiability assumptions in Assumption 3.1 and results in significant bias for the oracle models. We first fit the ILB, VAE based LVMs and regression baselines to the resulting datasets and then compared their performance in the online setting.

As can be seen in Figure 6 the oracle based models perform the worst with increasing noise. The regression model also struggles to learn and has a strong bias. LVM based VAE models perform the best compared to ILB based models. This is also reflected in the performance of model fitting (see Table 3).

We also observed that the FPG, for both ILB and VAE, was able to adapt to the increasing changes in the noise compared to CPG due to being able to trade-off the LVM estimation with the reward signal. Moreover, we see the benefit of exploration clearly highlighted here as FPG-TS outperformed both algorithms.

E.2 Out of distribution experiments

In this set of experiments we sampled out of distribution instances for the bandit algorithms. The results in Figure 7 show the difference of out of distribution generalization between the LVM and a regression model for increasing difference in $\Delta z = 1, 2$, and 4 . FPG, CPG, and regression models

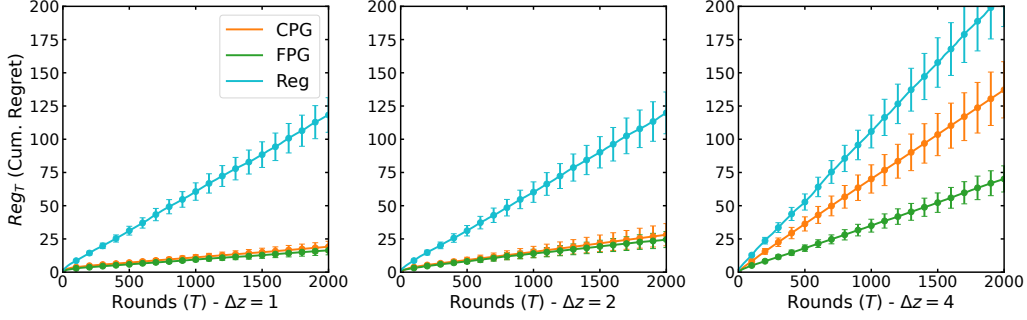
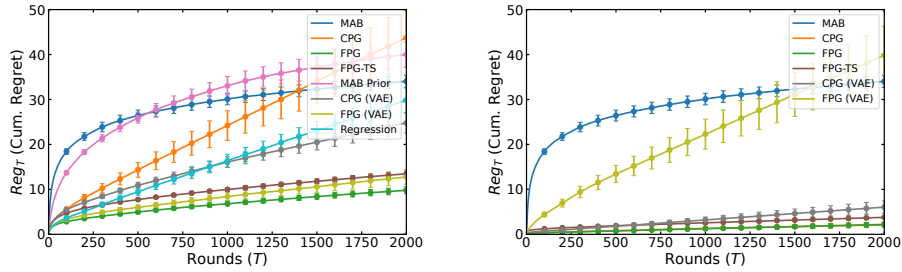


Figure 7: Expected cumulative for bandit algorithms for out of distribution generalization with means $\Delta z = 1, \Delta z = 2, \Delta z = 4$. Error bars indicate one standard error across 200 seeds.



(a) ADCB dataset with latent noise $\mathcal{N}(0, 0.1)$ (b) ADCB with latent noise $\mathcal{N}(0, 0.1)$ with *Age* related variable removed from the dataset.

Figure 8: Expected cumulative for bandit algorithms respective ADCB dataset with latent noise $\mathcal{N}(0, 0.1)$. Error bars indicate one standard error across 200 seeds.

show an increase in bias while LVM based models outperforms the baseline regression in every case. FPG model is able to generalize better compared to CPG due to using the signal in the reward.

E.3 Noise in the latent distribution and ADCB performance

In order to see the influence of the noise in the latent state, we increased the latent noise in the ADCB dataset to $\mathcal{N}(0, 0.1)$ from $\mathcal{N}(0, 0.02)$ in the main paper. We refit the LVM models and present in Figure 8a the results of the bandit algorithms. This makes the latent recovery much harder and puts the LVM models, especially CPG, at a disadvantage. As the reward noise is not affected, models that ignore the context such as MAB is not affected.

We see in Figure 8a that VAE model performs better compared to ILB based models in online, and in test performance in Table 4. We notice that this may be due to the *Age* variable in the ADCB dataset which has unique value for each patient making it trivial to predict the patient index (*C* in 4). After removing the *Age* variable from the dataset and refitting the LVMs, we measured the performance. We noticed a considerable increase in test results and bandit performance the results are in Figure 8b.

E.4 Nonlinear reward model

In Assumption 3.1 and Theorem 3.4 we assume linearity for the function θ determines the rewards from the latent state Z_i . This assumption is indeed useful as it allows for exploration by giving a close-form result for the posterior for FPG. However, our ILB algorithm also works when we allow for θ to be nonlinear. In Figure 9 we used a randomly initialized two layered MLP with leaky ReLU activations for the reward function θ . During the offline phase, we fit a four layered MLP to the estimated Z_i . For the fitted MLP we used leaky ReLU activations except for the final layer, which had no activations. For training we used Adam optimizer with learning rate 0.001 and weight decay 0.0001, and trained until convergence. For the offline stage, we only used the greedy strategy with

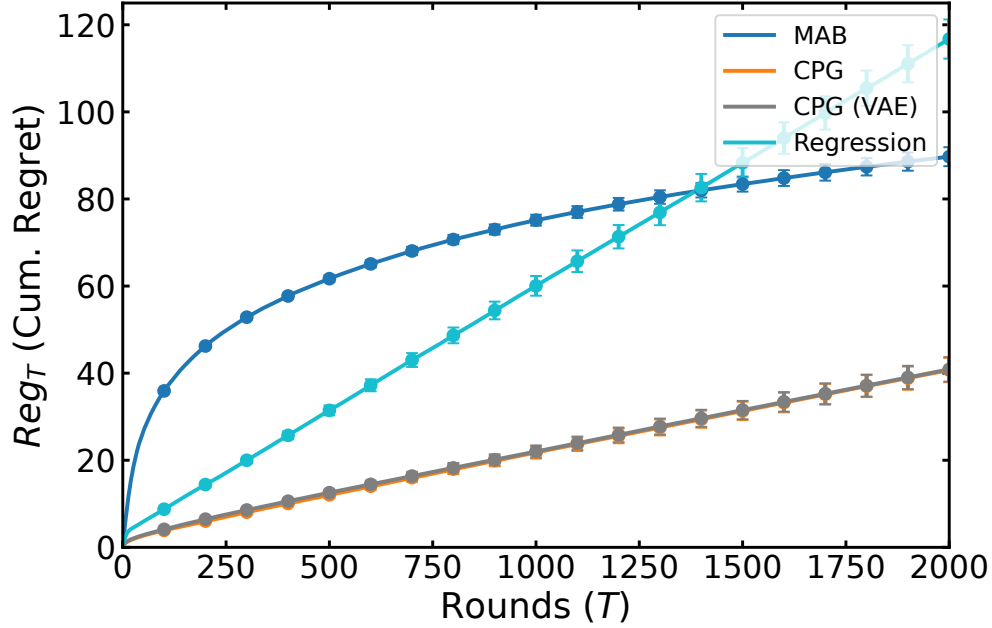


Figure 9: Expected cumulative regret plot regret for MAB, Regression and CPG algorithms for the nonlinear reward function. The error bars indicate one standard error computed across 1000 seeds.

CPG. The results show the effectiveness of our approach compared to the regression baseline. VAE based CPG performs similarly to our approach when compared to the linear case Figure 4.

E.5 Experiments under changing number of arms

The results in Figure 10 show the performance of LVM based CPG and FPG models compared to oracle based CPG and FPG and a Thompson sampling based MAB. MAB converges each time with slower convergence time to oracle and LVM based models. Oracle based models always converge to the best arm but need longer time for convergence due to the increasing difficulty of distinguishing the best arm. LVM based models on the other hand start to show a bias with increasing number of arms. This is an example of variance in the training time contributing to a bias in inference time.

E.6 Generalization to exponential family

We mention in Assumption 3.1 that the conditional distribution of the noise in the latent state $\eta_{i,t} \sim p(Z_{i,t}|Z_i)$ can come from any symmetric exponential family distribution. In Figure 11, we conduct experiments where the stationary noise in the latent state is distributed with respect to Laplace and uniform distributions in order to show model performance exponential family noise. LVM based models perform poorly due to the high variance of the uniform distribution, but outperform the Gaussian case for the tightly concentrated Laplace distribution. The results are comparable to having different levels of noise in the latent state.

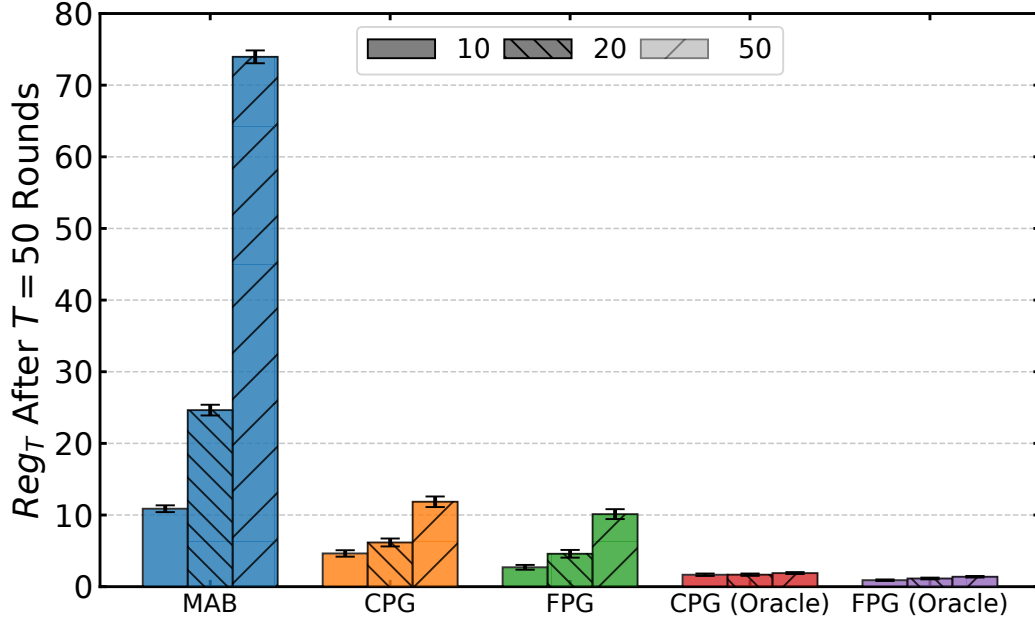


Figure 10: Expected cumulative regret for bandit algorithms in the cases of $K = 10$, $K = 20$, and $K = 50$ arms. Error bars show 1 standard error computed across 1000 seeds.

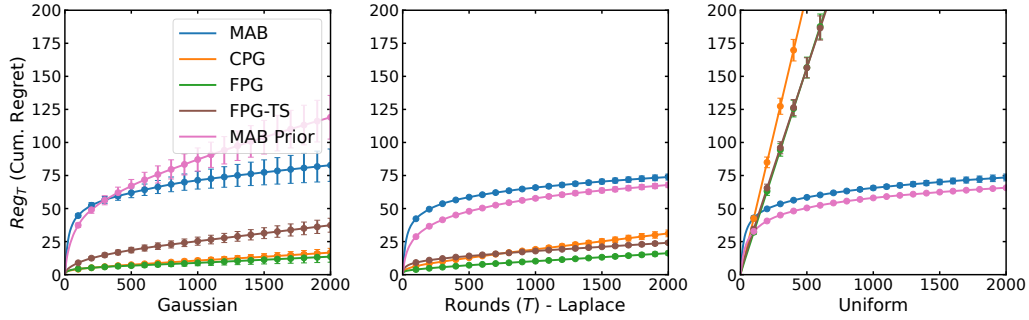


Figure 11: Expected cumulative regret plot regret for different exponential family noise. The error bars indicate one standard error computed across 1000 seeds.

F Synthetic example for linear contextual bandits with a stationary context

In our setting, since Z_i does not change, whichever action a^* that yields the highest expected reward for Z_i is optimal forever. Although the learner does observe a context X_t , without access to a LVM, instantaneous X_t does not provide additional information about the particular value of Z_i , so there is no reason to adapt the action based on X_t as in contextual bandits.

In effect, in this setting, since the conditional reward models θ_A are stationary: For a given Z_i , without access to a LVM, the only task would be to estimate their individual reward distributions θ_A^i , as $\hat{\theta}_A^i$, then select the optimal action a^* :

$$a^* = \arg \max_{a \in \mathcal{A}} \hat{\theta}_A^i,$$

which is exactly a non-contextual multi-armed bandit problem.

An extreme example of this is when the observed context X_i per instance i is stationary for all $t \in [T]$ with a fixed $\theta_A \in \mathbb{R}^{|\mathcal{A}| \times d}$, for d -dimensional context. We illustrate this empirically with a synthetic example:

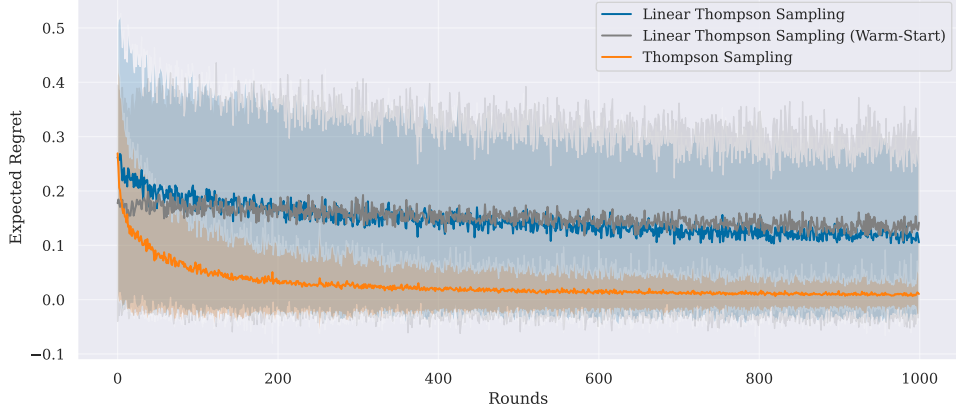


Figure 12: Synthetic example comparing linear contextual bandits for stationary context. $K = 10, d = 5, 500$ warm-start samples

Synthetic arm parameters:

$$\theta_{a,d} \sim \mathcal{U}(0.3, 0.8), \quad \epsilon_{a,d} \sim \mathcal{N}(0, 0.25), \quad \forall a \in \mathcal{A}$$

Synthetic context:

$$X_i \sim \mathcal{N}(\mu, \Sigma), \quad \forall i \in \{1, 2, \dots, N\}.$$

$$\mu = \begin{bmatrix} 0.5 \\ 0.5 \\ \vdots \\ 0.5 \end{bmatrix} \in \mathbb{R}^d, \quad \Sigma = 0.1\mathbf{I}_d + 0.05 \cdot \text{triu}(\mathbf{1}_{d \times d}, 1) + 0.05 \cdot \text{tril}(\mathbf{1}_{d \times d}, -1),$$

Where:

- $0.1\mathbf{I}_d$: Diagonal matrix with variance 0.1.
- $0.05 \cdot \text{triu}(\mathbf{1}_{d \times d}, 1)$: Upper triangular part (excluding diagonal) filled with 0.05.
- $0.05 \cdot \text{tril}(\mathbf{1}_{d \times d}, -1)$: Lower triangular part (excluding diagonal) filled with 0.05.

As seen in Figure 12, a non-contextual Thompson sampling [50, 43] algorithm outperforms its contextual [1] counterpart. We also include a warm-started Thompson sampling algorithm [33] which suffers the same fate. Warm-started Thompson sampling however converges faster than the not warm-started contextual Thompson sampling, although the non-optimal convergence for both is fairly similar compared to the non-contextual Thompson sampling.

G Conditional Reward modeling in ADCB from Average Treatment Effects

We aim to model a conditional treatment effect function $\text{ATE}_a(z)$ for each treatment a such that the expected treatment effect over the distribution of a continuous latent state $Z = Z^\dagger$ (where Z^\dagger is the continuous component of the latent state in ADCB) matches a predefined set of average treatment effects (ATEs). We'd also like to have heterogeneity of the treatments over Z . We model this on a latent state whose distribution is bimodal as shown in Figure 13.

G.1 Gaussian Mixture Model

Given our continuous latent state Z , its distribution can be expressed as a Gaussian Mixture Model (GMM) with two components:

$$p(Z) = \lambda_1 \mathcal{N}(\mu_1, \sigma_1^2) + \lambda_2 \mathcal{N}(\mu_2, \sigma_2^2)$$

where:

- $\lambda_1 = 0.572$ and $\lambda_2 = 0.428$ are the mixture weights with $\lambda_1 + \lambda_2 = 1$,
- $\mu_1 = 0.0979$ and $\mu_2 = 0.1986$ are the means of the Gaussian components,
- $\sigma_1^2 = 0.000541$ and $\sigma_2^2 = 0.000752$ are the variances of the Gaussian components.

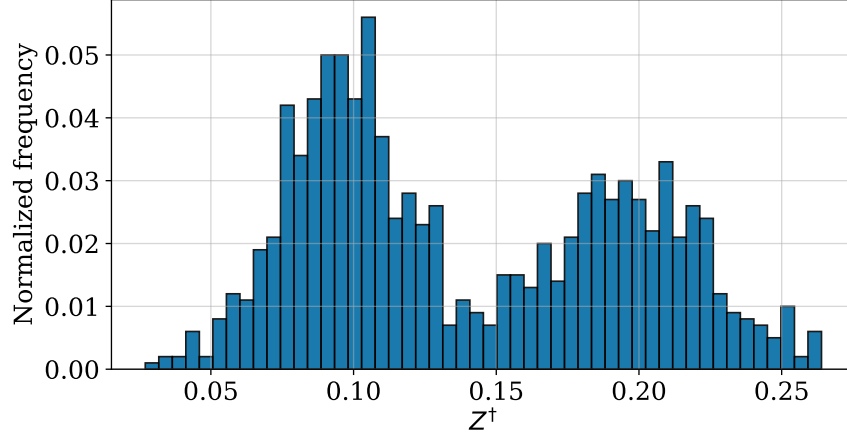


Figure 13: Histogram over 50 bins of the bimodally distributed continuous component of the latent state in ADCB

G.2 Expected Value of Z

The expected value of the latent state Z under this bimodal distribution is given by:

$$\mathbb{E}[Z] = \lambda_1 \mu_1 + \lambda_2 \mu_2$$

Substituting the values, we find:

$$\mathbb{E}[Z] = (0.572)(0.0979) + (0.428)(0.1986) \approx 0.1403$$

G.3 Heterogeneous Treatment Effect Model

The treatment effect for each treatment a is assumed to be a linear function of Z :

$$\text{ATE}_a(Z) = \alpha_a Z + \gamma_a$$

where α_a and γ_a are treatment heterogeneity parameters to be determined. The values of γ_a are chosen and fixed as:

$$\gamma = [0, -0.5, -1, -0.5, -2, -3.5, -1, -2.9]$$

G.4 Expected Treatment Effect

The expected treatment effect for each treatment a over the distribution of Z is given by:

$$\mathbb{E}[\text{ATE}_a(Z)] = \mathbb{E}[\alpha_a Z + \gamma_a] = \alpha_a \mathbb{E}[Z] + \gamma_a$$

G.5 Matching Expected Treatment Effects

We want the expected treatment effect for each treatment a to match a predefined average treatment effect $A_\Delta(a)$. We use 8 treatments with given values for A_Δ :

$$A_\Delta = [0, 1.95, 2.48, 3.03, 3.20, 2.01, 1.29, 2.69]$$

This gives:

$$\alpha_a \mathbb{E}[Z] + \gamma_a = A_\Delta(a)$$

We can solve for α_a as:

$$\alpha_a = \frac{A_\Delta(a) - \gamma_a}{\mathbb{E}[Z]}$$

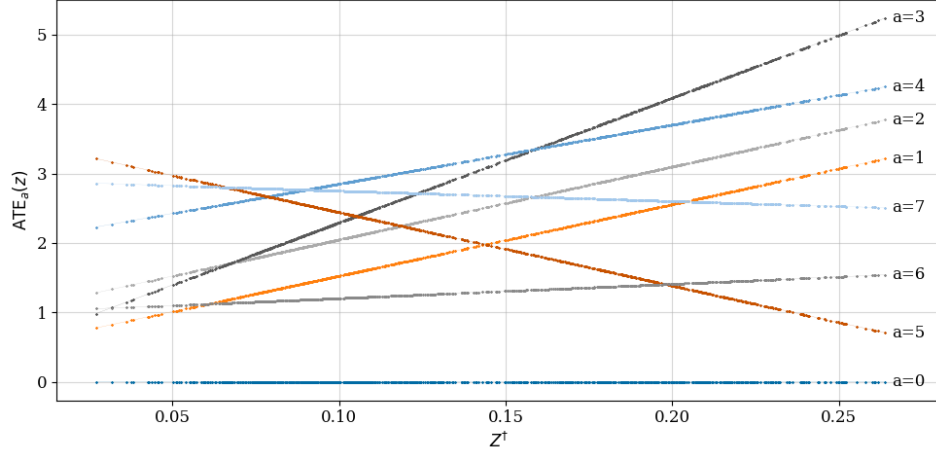


Figure 14: Conditional linear reward models in ADCB with heterogeneity over the latent state.

G.6 Matching Expected Treatment Effects with Noisy ATEs

To account for noise in the treatment effect observations, we introduce a level-variable additive Gaussian noise $\zeta_a \sim \mathcal{N}(0, \sigma^2)$:

$$\alpha_a \mathbb{E}[Z] + \gamma_a = A_{\Delta}(a) + \zeta_a$$

Solving for α_a , we find:

$$\alpha_a = \frac{A_{\Delta}(a) + \zeta_a - \gamma_a}{\mathbb{E}[Z]}$$

For a given value of z , the conditional treatment effect is then computable as:

$$\text{ATE}_a(z) = \alpha_a z + \gamma_a - \zeta_a$$

Using $\text{ATE}_a(z), \forall a \in \mathcal{A}$ as a conditional reward models gives us a model of $\mathbb{E}[R \mid Z = z, A = a] = \mathbb{E}[\text{ATE}_a(z)]$.

The resulting conditional reward models are illustrated in Figure 14.

Table 4: Complete LVM fitting results. L layers in the MLP, T_o time steps.

Synthetic Data					
L	T_o	Model	MCC_Z	R_R^2	% a^*
2	100	LVM	0.89	0.75	79
2	200	LVM	0.92	0.76	82
2	300	LVM	0.91	0.75	87
4	100	LVM	0.91	0.72	76
4	200	LVM	0.90	0.75	82
4	300	LVM	0.91	0.74	82
<hr/>					
2	100	VAE	0.94	0.69	70
2	200	VAE	0.93	0.72	88
2	300	VAE	0.94	0.70	72
4	100	VAE	0.87	0.43	40
4	200	VAE	0.91	0.43	48
4	300	VAE	0.91	0.51	52
<hr/>					
2	100	Regression	-	0.70	61
2	200	Regression	-	0.75	69
2	300	Regression	-	0.72	73
4	100	Regression	-	0.50	29
4	200	Regression	-	0.61	44
4	300	Regression	-	0.59	55
<hr/>					
ADCB					
L	T_o	Model	MCC_Z	R_R^2	% a^*
2	100	LVM	-	0.92	88
2	200	LVM	-	0.92	89
2	300	LVM	-	0.92	87
4	100	LVM	-	0.91	86
4	200	LVM	-	0.90	78
4	300	LVM	-	0.91	82
<hr/>					
2	100	VAE	-	0.94	95
2	200	VAE	-	0.94	97
2	300	VAE	-	0.94	95
4	100	VAE	-	0.94	95
4	200	VAE	-	0.94	96
4	300	VAE	-	0.94	95
<hr/>					
2	100	Regression	-	0.95	89
2	200	Regression	-	0.95	92
2	300	Regression	-	0.95	93
4	100	Regression	-	0.89	51
4	200	Regression	-	0.95	90
4	300	Regression	-	0.95	93

H LVM Results

Complete results on the test set for fitting of LVM, VAE, and Regression baselines for ADCB and LVM datasets Table 4.

I Experimental Setup

Training details for LVM We use an MLP with maxout activation functions for the feature extractor f . We select $L = 2$ and $L = 4$ layered models equal to different settings described in the data generating process, with hidden dimensions equal to dimensionality of Z_i . For the LVM we do a two-stage training: First, we freeze the MLP weights and only train the linear classifier, and then we train MLP and the classifier together. We train the MLP using SGD with momentum and ℓ_2 -regularization with initial learning rate of 0.01, exponential decay of 0.1, and momentum 0.9. We run each experiment across 10 different seeds.

Training details for VAE We select $L = 2$ and $L = 4$ layered encoder and decoder models equal to different settings described in the data generating process, with hidden dimensions equal to dimensionality of Z_i . We train the model with KL-divergence reconstruction loss. For training we use Adam optimizer with a weight decay of 0.001 and a learning rate of 0.001. We train for 100 epochs with early stopping based on validation loss with a patience of 5 epochs. We run each experiment across 10 different seeds.

Details for the regression baseline For the regression baseline, we use a TARNet architecture [47] with a GRU encoder using $L = 2$ and $L = 4$ layers for different settings with a hidden feature size of 64, selected on the validation set. We train the model with MSE loss on observed rewards using Adam optimizer with weight decay of 0.001 and an exponentially dampening learning rate starting at 0.01 with decay factor 0.1. We for 100 epochs, each with increasing sequence length and a batch size of 100 instance sequence and perform early stopping based on R^2 for observed rewards. We run each experiment across 10 different seeds.

Further training details We used an NVIDIA T4 GPU for producing most of the training for this work. Most expensive experiments took at most 2 hours train for 10 seeds. For bandit algorithms we used 10 Intel(R) Xeon(R) Gold 6338 CPUs and ran seeds in parallel with a cost of about 5 CPU hours for 200 seeds.

Impact Statement

This paper presents work whose goal is to advance the decision-making through machine learning. Any application of automated decision-making must be made with caution and sufficient guard rails appropriate for the specific problem. Our work is primarily methodological and does not have direct practical implications on healthcare or other domains.